J. Fluid Mech. (1993), *vol.* 257, *pp.* 403–420

Non-axisymmetric motion of rigid closely fitting particles in fluid-filled tubes

By T. W. SECOMB AND R. HSU
Department of Physiology, University of Arizona, Tucson, AZ 85724, USA

(Received 1 March 1991 and in revised form 14 June 1993)

We consider non-axisymmetric motion of a rigid particle in a cylindrical fluid-filled tube, with negligible inertial effects. The particle is assumed to fit closely in the tube, and lubrication theory is used to describe the fluid flow in the narrow gap between the particle and the tube wall. The solution to the Reynolds lubrication equation and the components of the resistance matrix are expressed in terms of a Green's function. For the case in which the gap is almost uniform, the Green's function is expanded as a power series in a small parameter δ, characteristic of the variations in gap width, and the first two terms are obtained.

The velocity of a freely suspended axisymmetric particle driven by a pressure difference along the tube is deduced from the resistance matrix. According to the results at first order in δ, in general the particle moves transversely with a constant velocity. In the absence of higher-order effects, it would eventually collide with the wall. Motion along the tube axis is a neutrally stable solution to the equations of motion at first order. However, if effects at second order in δ are included, motion of an axisymmetric particle along the tube axis is stable or unstable depending on its shape. Generally, if the particle is narrower near the front than near the rear, and the width near the middle is at least as large as the mean of the widths near the front and rear, then its motion is stable. Numerical calculations (not restricted to small δ) confirm these results for axisymmetric particles, and show that a non-axisymmetric shape similar to a red blood cell has a stable equilibrium position in the tube.

1. Introduction

A number of physical systems involve the motion of freely suspended particles through fluid-filled passages, when the particle size is comparable with the diameter or width of the pathway, and when inertial effects may be assumed negligible. Biological examples include the motion of red and white blood cells through capillaries and the motion of solute molecules through narrow pores in vessel walls or other structures. More generally, flow of suspensions or two-phase fluids through porous media often results in systems of this type.

Most theoretical studies of such systems have considered non-interacting rigid spherical particles in a cylindrical tube, or have assumed that the particles are axisymmetric and located on the axis of the tube. In both cases, symmetry arguments show that the particle moves parallel to the tube axis, without migrating in the radial direction. In the case of rigid spheres, this conclusion depends on the linearity of the governing equations, and radial migration is possible if inertial effects are present, if the particle is deformable, or if the suspending fluid is non-Newtonian (Leal 1980).

Analyses of the motion of a single rigid spherical particle within a cylindrical tube were reviewed by Happel & Brenner (1973), who present a theory for the case when the

radius of the sphere is small relative to the tube radius. The case of a closely fitting sphere was analysed by Christopherson & Dowson (1959) using lubrication theory, and Bungay & Brenner (1973) using a singular perturbation approach. As pointed out above, no radial migration is predicted.

Numerous studies have been made of the motion of axisymmetric but non-spherical particles moving along the tube axis. Both rigid and deformable particles have been considered. Wakiya (1957) and Chen & Skalak (1970) developed analytic solutions for rigid spheroidal particles. Zarda, Chien & Skalak (1977) used a finite-element numerical method to describe the motion of deformable red blood cells. The observation that red and white blood cells have dimensions comparable with capillary diameters and are often closely fitting led to analyses using lubrication theory, including Barnard, Lopez & Hellums (1968), Lighthill (1968), Tözeren & Skalak (1978), and Secomb *et al.* (1986).

Observed blood cell shapes in microvessels are frequently non-axisymmetric. Also, cells often enter a vessel segment in off-axis positions. Few analyses have been made of asymmetric motion of highly non-spherical particles in tubes. Secomb & Skalak (1982) developed a two-dimensional model for capillary flow of a very flexible, asymmetric cell, using lubrication theory. Sugihara-Seki, Secomb & Skalak (1990) considered a two-dimensional model for two-file flow of cells with prescribed shapes, using a finite-element method. Hsu & Secomb (1989) used lubrication theory to analyse the motion of non-axisymmetric red blood cells in cylindrical capillaries, and determined the cell orientation and transverse displacement at which the conditions of zero lift, drag and torque were satisfied, for given cell shape and tube diameter. However, no systematic study was made of the stability of these equilibrium positions, or of the trajectories followed by cells starting from different initial positions.

The goal of the present work is to determine trajectories of non-spherical particles flowing along tubes, when the particle is not axisymmetrically located, and to analyse the stability of motion of axisymmetric particles on the tube axis. For simplicity, we assume that the particles are rigid. The results represent a first step towards analysing the motion of flexible particles.

We use lubrication theory, under the assumption that the particle fits closely in the tube. The equations governing the motion of the suspending fluid around the particle are then greatly simplified, compared with other approaches described above.

The ability of lubrication theory to describe particle-to-wall interactions in Stokes flow depends on the configuration being considered, and particularly on the size of the narrow-gap region relative to the overall particle size. In the case of a sphere moving adjacent to a plane wall, lubrication theory does not provide good approximations to the force on the sphere (Goldman, Cox & Brenner 1967). The narrow-gap region represents only a small part of the sphere's surface, and even though large stresses occur there, the resultant forces and torques do not dominate those generated elsewhere. However, lubrication theory does yield good approximations for the pressure drop across a sphere moving on the axis of a cylindrical tube, even when gap width is not very small (Hochmuth & Sutera 1970; Secomb *et al.* 1986). In that case, the lubrication region is a band around the circumference of the sphere, and represents a larger fraction of the sphere's surface than in the case of a sphere adjacent to a plane wall. In the case of an elongated closely fitting particle in a tube, the lubrication region extends over an even larger fraction of the particle's surface. Since the largest stresses are generated in the lubrication region, it follows that lubrication theory should yield useful estimates of resultant forces for a broad class of closely fitting particle shapes in fluid-filled tubes.

2. The lubrication equation

The configuration is indicated in figure 1. A particle fits closely within a cylindrical tube of radius r_0 filled with an incompressible Newtonian fluid with viscosity μ, and moves along the tube with velocity of order u_0. At this point, we make all variables non-dimensional with respect to u_0, r_0 and μ, unless otherwise stated. For instance, pressures and stresses are non-dimensionalized with respect to $\mu u_0/r_0$.

The particle surface is almost cylindrical in the region in which it closely approaches the wall of the tube. We assume that the gap width in the region is of order $\epsilon \ll 1$. It is convenient to introduce cylindrical coordinate systems (r, θ, z) fixed in the particle frame, and (r', θ', z') fixed in the tube frame. The tube wall is then located at $r' = 1$. The z'-axis is not necessarily parallel to the z-axis, but lies within a distance ϵ of the z-axis over the length of the particle. Then the particle surface and the tube wall are described by

$$r = 1+\epsilon\xi_p(z,\theta) \quad \text{and} \quad r = 1+\epsilon\xi_w(z,\theta,t) \tag{2.1}$$

respectively, where ξ_p and ξ_w are $O(1)$.

We assume that inertial effects are negligible, so that the fluid velocity $\boldsymbol{u} = (u_r, u_\theta, u_z)$ and the pressure p satisfy the Stokes equations

$$0 = -\nabla p+\nabla^2\boldsymbol{u} \tag{2.2}$$

and

$$\nabla\cdot\boldsymbol{u} = 0. \tag{2.3}$$

If the length of the particle is of order 1, then (2.3) implies that $u_r = O(\epsilon)$, and the z-component of (2.2) implies that $p = O(\epsilon^{-2})$. However, the r-component of (2.2) implies that variations in p across the gap (in the r-direction) are of order ϵ^0. Therefore, the pressure is uniform across the gap at the two leading orders in ϵ (ϵ^{-2} and ϵ^{-1}).

We introduce scaled variables as follows:

$$\xi = (r-1)/\epsilon, \quad P = \epsilon^2 p, \quad U_r = \epsilon^{-1}u_r, \quad U_\theta = u_\theta, \quad U_z = u_z. \tag{2.4}$$

At leading order in ϵ, the z- and θ-components of (2.2) yield

$$\frac{\partial P}{\partial z} = \frac{\partial^2 U_z}{\partial\xi^2}, \quad \frac{\partial P}{\partial\theta} = \frac{\partial^2 U_\theta}{\partial\xi^2}. \tag{2.5}$$

We suppose that the wall moves with velocity $\boldsymbol{u}_w(z,\theta,t) = (\epsilon U_{rw}, U_{\theta w}, U_{zw})$ in the particle frame. From (2.1), the no-slip boundary conditions at the particle and tube surfaces are

$$\boldsymbol{u} = 0 \quad \text{when} \quad \xi = \xi_p \quad \text{and} \quad \boldsymbol{u} = \boldsymbol{u}_w \quad \text{when} \quad \xi = \xi_w. \tag{2.6}$$

Using (2.5), the velocity in the gap may be computed in terms of the pressure gradient:

$$\left.\begin{aligned} U_z &= -\frac{1}{2}\frac{\partial P}{\partial z}(\xi-\xi_p)(\xi_w-\xi)+U_{zw}\frac{\xi-\xi_p}{h}, \\ U_\theta &= -\frac{1}{2}\frac{\partial P}{\partial\theta}(\xi-\xi_p)(\xi_w-\xi)+U_{\theta w}\frac{\xi-\xi_p}{h}, \end{aligned}\right\} \tag{2.7}$$

where $h(z,\theta,t) = \xi_w-\xi_p$ is the gap width. The volume flux in the gap between the particle and the wall is given at leading order by $Q_z(z,\theta,t)$ and $Q_\theta(z,\theta,t)$ where

$$Q_\theta = \int_{\xi_p}^{\xi_w} U_\theta\,\mathrm{d}\xi \quad \text{and} \quad Q_z = \int_{\xi_p}^{\xi_w} U_z\,\mathrm{d}\xi. \tag{2.8}$$

Applying the continuity condition (2.3) gives

$$\frac{\partial Q_z}{\partial z}+\frac{\partial Q_\theta}{\partial\theta}+\frac{\partial h}{\partial t} = 0. \tag{2.9}$$

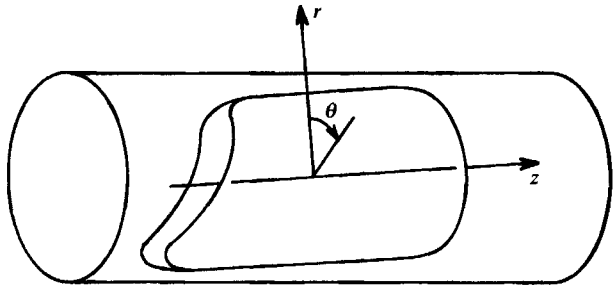

FIGURE 1. Particle in a tube, with coordinates fixed in the particle.

Evaluating (2.8) and substituting in (2.9) yields the well-known Reynolds equation of lubrication theory (Cameron 1966, p. 61), which we write in the form

$$\mathrm{L}(P) = f(z, \theta, t), \tag{2.10}$$

where

$$\mathrm{L}(P) = \frac{\partial}{\partial z}\left(h^3 \frac{\partial P}{\partial z}\right) + \frac{\partial}{\partial \theta}\left(h^3 \frac{\partial P}{\partial \theta}\right)$$

and

$$f(z, \theta, t) = 12\frac{\partial h}{\partial t} + 6\frac{\partial}{\partial z}[hU_{zw}] + 6\frac{\partial}{\partial \theta}[hU_{\theta w}].$$

The pressure P is periodic in θ with period 2π, and takes a prescribed value at each end of the lubrication region. We assume that the region of narrow gap is given by $S = \{-\pi \leqslant \theta \leqslant \pi, z_-(\theta) \leqslant z \leqslant z_+(\theta)\}$. Since the driving pressure must balance the shear stress on the particle, which is $O(\epsilon^{-1})$, the driving pressure is also $O(\epsilon^{-1})$. The fluctuations in pressure within the gap are therefore generally an order of ϵ^{-1} larger than the overall pressure change, as is often the case in lubrication. Consequently, the boundary conditions are, at leading order,

$$P(z_-(\theta), \theta) = P(z_+(\theta), \theta) = 0, \quad P(z, -\pi) = P(z, \pi), \quad \frac{\partial P(z, -\pi)}{\partial \theta} = \frac{\partial P(z, \pi)}{\partial \theta}. \tag{2.11}$$

3. The stability of axial particle motions: qualitative arguments

Before proceeding with the detailed analysis of (2.10), we present qualitative arguments regarding the stability of the motion of an axisymmetric particle along the tube axis. The conclusions of this section will be confirmed and extended by the subsequent analyses (§§4–7). Similar qualitative arguments are given by Boyd (1964), for the cases noted below. The theory of thrust pad bearings (Cameron 1966) is also relevant.

For this discussion, we assume that an axisymmetric particle is placed in the tube, and constrained to move with velocity U_0 parallel to the tube axis without rotation. We suppose that the particle axis may be displaced or rotated relative to the tube axis, with the two axes coplanar. The resulting particle–tube configuration has mirror symmetry about the plane containing the axes. We consider the resultant forces and/or torques on the particle, resulting from the pressure distribution in the narrow gap surrounding the particle. According to the scalings above, the resultant forces due to pressure variations in the gap dominate those due to shear stresses. From the symmetry of the configuration, these resultant forces act in the symmetry plane. To further simplify the problem, we assume that the particle is sufficiently cylindrical and the displacement of

the particle is sufficiently small that the gap width h is nearly uniform over the surface of the particle.

Under these assumptions, (2.10) becomes

$$\frac{\partial}{\partial z}\left(h^3\frac{\partial P}{\partial z}\right)+\frac{\partial}{\partial \theta}\left(h^3\frac{\partial P}{\partial \theta}\right)=-6U_0\frac{\partial h}{\partial z} \tag{3.1}$$

with homogeneous, θ-periodic boundary conditions. Since h is nearly uniform, the left-hand side of (3.1) is approximately equal to $h^3\nabla^2 P$ (corresponding to a Hele-Shaw flow). Since the boundary conditions are homogeneous, well-known properties of the Laplacian imply that negative values of $\partial h/\partial z$ correspond to a source term and generate positive pressure P, and vice versa. Furthermore, the amplitude of the pressure fluctuations generated for a given $\partial h/\partial z$ must increase as h decreases (approximately in proportion to h^{-3}). These two qualitative properties of (3.1) provide a basis for predicting the stability of axial particle motions.

Several axisymmetric cell shapes are shown schematically in figure 2, as they intersect the symmetry plane. We consider the pressures generated in the upper and lower gaps in this plane, which are representative of the pressure generated around the upper and lower parts of the particle circumference. The particle motion is from left to right in each case.

First, we consider a cylindrical particle. If the particle is displaced from the axis without rotation (figure 2*a*), no pressure changes are generated according to this approximation. If the particle is rotated (figure 2*b*), the pressure increases in that part of the gap that is wider at the front than at the rear, and decreases on the opposite side of the particle. The particle will therefore tend to move transversely in the direction indicated (Boyd 1964). As figure 2(*d*,*f*,*h*) indicates, this characteristic is retained even if the particle is not cylindrical. We shall show later that the particle motion at each instant is approximately parallel to the bisector of the particle axis and the tube axis.

Next, we consider a tapered particle, narrower at the front than at the rear. Positive pressures are generated on all sides of the particle. If it is displaced sideways (figure 2*c*), higher pressures are generated on the side where the gap is narrower, tending to restore the particle to the axis (Boyd 1964). (For further discussion of this case see the paragraph on third-order effects in §6). Similarly, if the particle is rotated (figure 2*d*), a torque that tends to realign the particle is superimposed on the transverse force. From these arguments, we may guess that particle motion on the axis is stabilized by such a taper, as will be confirmed later. Conversely, a tapered particle that is wider at the front than the rear will be unstable with respect to both displacement and rotation, since large *negative* pressures will be generated where the gap is narrowest.

Figure 2(*e*) shows a particle that is wider at the ends than the middle. Sideways displacement of such a particle results in a torque, and particle rotation in the direction of the torque causes the particle to move further from the axis (figure 2*f*). We conclude that motion of such a particle along the tube axis in either direction is likely to be unstable.

Finally, we consider a particle that is wider at the middle than the ends (figure 2*g*). Transverse displacement of this particle generates a torque opposite to that in figure 2(*e*). Rotation of the particle in the direction of the torque will produce a transverse force tending to restore the particle to the axis (the converse of the case shown in figure 2*h*). However, this process involves a time lag, suggesting the possibility of oscillatory behaviour.

Clearly, a detailed analysis is required to test, extend, and make quantitative the above predictions. Such an analysis follows.

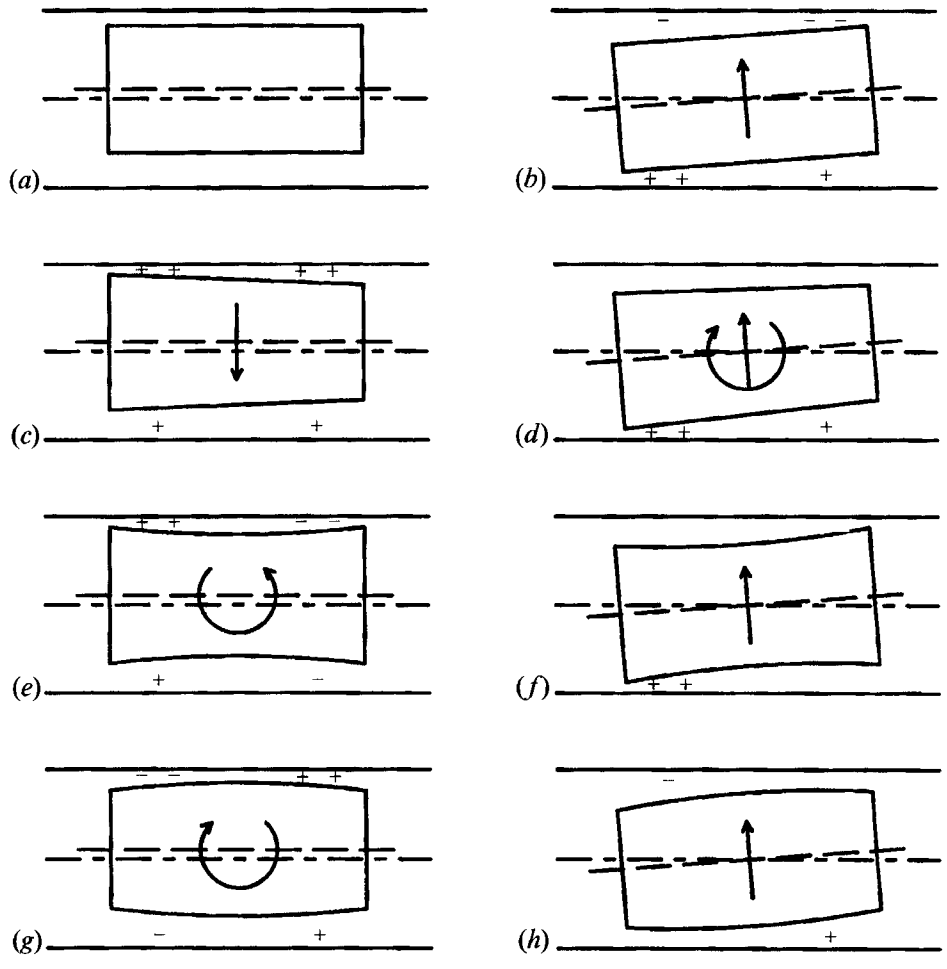

FIGURE 2. Schematic representation of pressure distributions and resultant forces and torques generated by transverse displacements (a, c, e, g) or rotations (b, d, f, h) of axisymmetric particles moving to the right in a cylindrical tube. Positive pressures are denoted by + and negative pressures by −. Where the gap is relatively narrow, the magnitude of the pressure variation is large, as indicated by + + or − −. See text for further explanation.

4. Formulation of the problem and Green's function solution

4.1. *Geometry and kinematics*

To describe the relative motion of tube and particle, we introduce Cartesian coordinates (x, y, z) fixed in the particle, with the x-axis in the $\theta = 0$ direction of the (r, θ, z) system, and similarly Cartesian coordinates (x', y', z') fixed in the tube. We suppose that the origin of the tube coordinates is at $(\epsilon a, \epsilon b, c)$ and the tube (z') axis is parallel to $(\epsilon\alpha, \epsilon\beta, 1)$ in the particle frame (x, y, z). The x'-axis is assumed to be at an angle γ to the x-axis, i.e. parallel to $(\cos\gamma, \sin\gamma, -\epsilon\alpha\cos\gamma - \epsilon\beta\sin\gamma)$ in the (x, y, z) frame. The parameters a, b, c, α, β and γ are functions of time, and are $O(1)$ according to the assumptions already stated. Then

$$\left.\begin{aligned} x &= \cos(\gamma+\theta') + \epsilon a + \epsilon\alpha z' + O(\epsilon^2), \\ y &= \sin(\gamma+\theta') + \epsilon b + \epsilon\beta z' + O(\epsilon^2), \\ z &= c + z' - \epsilon\alpha\cos(\gamma+\theta') - \epsilon\beta\sin(\gamma+\theta') + O(\epsilon^2), \end{aligned}\right\} \tag{4.1}$$

i	V_i	W_i	F_i
1	V_x	$\cos\theta$	F_x
2	V_y	$\sin\theta$	F_y
3	V_z	$-\partial\xi_m/\partial z$	F_z
4	Ω_x	$-z\sin\theta$	T_x
5	Ω_y	$z\cos\theta$	T_y
6	Ω_z	$-\partial\xi_m/\partial\theta$	T_z

TABLE 1. The V_i and W_i in equation (4.9) and the F_i in (4.12)

and so the tube surface is given in particle coordinates by

$$\xi_w(z,\theta,t) = [a+\alpha(z-c)]\cos\theta+[b+\beta(z-c)]\sin\theta. \tag{4.2}$$

We let $(\epsilon V_x, \epsilon V_y, V_z)$ and $(\epsilon\Omega_x, \epsilon\Omega_y, \Omega_z)$ be the Cartesian components of the velocity and angular velocity of the particle relative to the tube, expressed in the particle coordinates. The velocity of a point (x,y,z) fixed in the tube is then

$$\boldsymbol{u} = -[(\epsilon V_x, \epsilon V_y, V_z)+(\epsilon\Omega_x, \epsilon\Omega_y, \Omega_z)\times(x,y,z)]. \tag{4.3}$$

Comparing this with the time-derivative of (4.1), we find the following conditions for consistency at leading order in ϵ:

$$\left.\begin{aligned} \frac{\mathrm{d}a}{\mathrm{d}t} &= -V_x-\Omega_y c+\Omega_z b, \quad \frac{\mathrm{d}b}{\mathrm{d}t} = -V_y+\Omega_x c-\Omega_z a, \quad \frac{\mathrm{d}c}{\mathrm{d}t} = -V_z, \\ \frac{\mathrm{d}\alpha}{\mathrm{d}t} &= -\Omega_y+\Omega_z\beta, \quad \frac{\mathrm{d}\beta}{\mathrm{d}t} = \Omega_x-\Omega_z\alpha, \quad \frac{\mathrm{d}\gamma}{\mathrm{d}\tau} = -\Omega_z. \end{aligned}\right\} \tag{4.4}$$

From (4.3), the leading-order components of tube wall velocity in cylindrical coordinates are

$$U_{\theta w} = -\Omega_z, \quad U_{zw} = -V_z, \quad U_{rw} = -V_x\cos\theta-V_y\sin\theta-(\Omega_y\cos\theta-\Omega_x\sin\theta)z. \tag{4.5}$$

Now, U_{rw} is the radial velocity of a point moving with the tube, while $\partial h/\partial t$ is evaluated at a constant value of z. Therefore, since the particle is at rest,

$$\frac{\partial h}{\partial t} = U_{rw}-U_{zw}\frac{\partial\xi_w}{\partial z}-U_{\theta w}\frac{\partial\xi_w}{\partial\theta}. \tag{4.6}$$

Equations (4.5) and (4.6) are substituted in the right-hand side of the lubrication equation (2.10), giving

$$f(z,\theta,t) = -12\left[V_x\cos\theta+V_y\sin\theta+(\Omega_y\cos\theta-\Omega_x\sin\theta)z-V_z\frac{\xi_m}{\partial z}-\Omega_z\frac{\partial\xi_m}{\partial\theta}\right], \tag{4.7}$$

where

$$\xi_m(z,\theta,t) = \tfrac{1}{2}[\xi_w(z,\theta,t)+\xi_p(z,\theta)]. \tag{4.8}$$

It is convenient to write (4.7) in the form

$$f(z,\theta) = -12\sum_{i=1}^{6} V_i W_i(z,\theta), \tag{4.9}$$

where V_i and W_i are as defined in table 1, and where the time dependence of all the variables is considered implicit from here on.

4.2. *Force and torque on the particle*

At leading order in ϵ, the components of stress in the fluid are

$$\sigma_{zz} = \sigma_{rr} = \sigma_{\theta\theta} = -\epsilon^{-2}P, \quad \sigma_{zr} = \epsilon^{-1}\frac{\partial U_z}{\partial \xi}, \quad \sigma_{r\theta} = \epsilon^{-1}\frac{\partial U_\theta}{\partial \xi}, \quad \sigma_{\theta z} = O(1) \tag{4.10}$$

and the unit vector normal to the particle is $(1, -\epsilon\partial\xi_p/\partial\theta, -\epsilon\partial\xi_p/\partial z)$. Therefore, the components of force per unit area exerted by the fluid on the particle are at leading order $(\epsilon^{-2}\tau_r, \epsilon^{-1}\tau_\theta, \epsilon^{-1}\tau_z)$, where, from (2.7)

$$\tau_r = -P, \quad \tau_\theta = -\frac{h}{2}\frac{\partial P}{\partial \theta} + \frac{U_{\theta w}}{h} + P\frac{\partial \xi_p}{\partial \theta}, \quad \tau_z = -\frac{h}{2}\frac{\partial P}{\partial z} + \frac{U_{zw}}{h} + P\frac{\partial \xi_p}{\partial z}. \tag{4.11}$$

The Cartesian components of total force and torque on the particle resulting from fluid stresses in the narrow-gap region may be written $(\epsilon^{-2}F_x, \epsilon^{-2}F_y, \epsilon^{-1}F_z)$ and $(\epsilon^{-2}T_x, \epsilon^{-2}T_y, \epsilon^{-1}T_z)$. To obtain the components, the Cartesian resultants of (4.11) are integrated over the gap. After some manipulation, it is found that

$$F_i = -\int_S P(z,\theta)\, W_i(z,\theta)\, \mathrm{d}S - V_i\, W_i', \tag{4.12}$$

where F_i are the components of force and torque as defined in table 1, W_i are the same functions that appeared in (4.9) and table 1, and

$$W_i' = \int_S \frac{1}{h}\mathrm{d}S \quad \text{if} \quad i = 3 \text{ or } 6; \qquad W_i' = 0 \quad \text{if} \quad i = 1, 2, 4 \text{ or } 5. \tag{4.13}$$

4.3. *Green's function solution.*

The solution to (2.10) and (2.11) is

$$P = \int_{S^*} G(z,\theta; z^*, \theta^*) f(z^*, \theta^*)\, \mathrm{d}S^*, \tag{4.14}$$

where the Green's function G satisfies

$$\mathrm{L}(G) = \delta(z - z^*)\, \delta(\theta - \theta^*) \tag{4.15}$$

and the boundary conditions (2.11). Using (4.9), therefore,

$$P(z,\theta) = -12 \sum_{i=1}^{6} V_i \int_{S^*} G(z,\theta; z^*, \theta^*)\, W_i(z^*, \theta^*)\, \mathrm{d}S^*. \tag{4.16}$$

Combining this with (4.12), we find that

$$F_i = \sum_{j=1}^{6} R_{ij}\, V_j,$$

where the *resistance matrix* R_{ij} is given by

$$R_{ij} = 12 \int_S \int_{S^*} G(z,\theta; z^*, \theta^*)\, W_i(z,\theta)\, W_j(z^*, \theta^*)\, \mathrm{d}S\, \mathrm{d}S^* - \delta_{ij}\, W_i' \tag{4.17}$$

and δ_{ij} denotes the Kronecker delta.

The operator L may be shown to be self-adjoint with respect to functions satisfying (2.11). It follows that the Green's function G is symmetric with respect to its arguments (z,θ) and (z^*,θ^*), and therefore that the matrix R_{ij} is symmetric. Other general properties of the resistance matrix are discussed by Happel & Brenner (1973, p. 178).

5. The Green's function for almost uniform gaps

In this section, we make two additional assumptions. We suppose that the front and rear boundaries of the lubrication region lie in planes perpendicular to the particle axis, i.e. that $z_-(\theta) = -l_0$ and $z_+(\theta) = l_0$, where l_0 is a constant. Also, we assume that the variations in the gap width are of order $\epsilon\delta$, where $\epsilon \ll \delta \ll 1$, so that higher-order $[O(\epsilon^2)]$ terms arising from lubrication theory terms may be neglected while $O(\epsilon\delta)$ terms arising from variations in gap width are included. According to this assumption, the departure of the particle from cylindrical shape, and the displacement of the particle axis from the tube axis, must be small compared to the gap width. The tube wall is located at $r = 1+\epsilon\delta\xi_{w1}$ and the particle surface is located at $r = 1-\epsilon+\epsilon\delta\xi_{p1}$. Consequently, we let

$$\left.\begin{gathered} a = \delta a_1, \quad b = \delta b_1, \quad \alpha = \delta\alpha_1, \quad \beta = \delta\beta_1, \\ h = 1+\delta h_1 \quad \text{where} \quad h_1 = \xi_{w1}-\xi_{p1}, \\ \xi_m = -\tfrac{1}{2}+\delta\xi_{m1} \quad \text{where} \quad \xi_{m1} = \tfrac{1}{2}(\xi_{w1}+\xi_{p1}). \end{gathered}\right\} \tag{5.1}$$

It is convenient to express h_1 as a Fourier series:

$$h_1 = \frac{1}{2}\sum_{p=-\infty}^{\infty} H_p(z)\,\mathrm{e}^{-\mathrm{i}p\theta}, \tag{5.2}$$

where H_p is complex for $p \neq 0$, with $H_{-p} = \bar{H}_p$.

With these assumptions, the Green's function may be expanded in powers of δ. We set

$$\left.\begin{gathered} G = G_0+\delta G_1+\ldots \quad \text{and} \quad \mathrm{L} = \mathrm{L}_0+\delta\mathrm{L}_1+\ldots, \\ \text{where} \qquad \mathrm{L}_0 = \frac{\partial^2}{\partial z^2}+\frac{\partial^2}{\partial\theta^2} \quad \text{and} \quad \mathrm{L}_1 = 3\frac{\partial}{\partial z}\left(h_1\frac{\partial}{\partial z}\right)+3\frac{\partial}{\partial\theta}\left(h_1\frac{\partial}{\partial\theta}\right). \end{gathered}\right\} \tag{5.3}$$

Then (4.15) gives at leading order

$$\mathrm{L}_0(G_0) = \delta(z-z^*)\,\delta(\theta-\theta^*). \tag{5.4}$$

We express G_0 as a Fourier series:

$$G_0 = \frac{1}{2}\sum_{m=-\infty}^{\infty} g_m(z,z^*)\,\mathrm{e}^{\mathrm{i}m(\theta-\theta^*)}, \tag{5.5}$$

where the real functions g_m satisfy $g_{-m} = g_m$ and

$$\frac{\partial^2 g_m}{\partial z^2}-m^2 g_m = \frac{\delta(z-z^*)}{\pi}. \tag{5.6}$$

The solutions satisfying the boundary conditions (2.11) are

$$\left.\begin{aligned} g_0(z,z^*) &= \begin{cases} -(l_0+z)(l_0-z^*)/2\pi l_0, & z < z^*; \\ -(l_0-z)(l_0+z^*)/2\pi l_0, & z > z^*; \end{cases} \\ g_m(z,z^*) &= \begin{cases} -\dfrac{\sinh[m(l_0+z)]\sinh[m(l_0-z^*)]}{m\pi\sinh[2ml_0]}, & z < z^*; \\ -\dfrac{\sinh[m(l_0-z)]\sinh[m(l_0+z^*)]}{m\pi\sinh[2ml_0]}, & z > z^*. \end{cases} \end{aligned}\right\} \tag{5.7}$$

At the next order, δ^1:

$$\mathrm{L}_0(G_1) = -\mathrm{L}_1(G_0). \tag{5.8}$$

Using the leading-order Green's function to invert L_0, and integrating by parts, we find that

$$G_1(z,\theta;z^*,\theta^*) = 3\int_{S'}\left[\frac{\partial}{\partial z'}G_0(z,\theta;z',\theta')\frac{\partial}{\partial z'}G_0(z',\theta';z^*,\theta^*) + \frac{\partial}{\partial \theta'}G_0(z,\theta;z',\theta')\frac{\partial}{\partial \theta'}G_0(z',\theta';z^*,\theta^*)\right]h_1(z',\theta')\,\mathrm{d}S'. \tag{5.9}$$

From (5.2) and (5.5), we deduce that

$$\left.\begin{aligned} G_1(z,\theta;z^*,\theta^*) &= \frac{3\pi}{4}\sum_{m=-\infty}^{\infty}\sum_{n=-\infty}^{\infty}\int_{-l_0}^{l_0}\Gamma_{mn}(z,z',z^*) \\ &\quad\times H_{m+n}(z')\,\mathrm{d}z'\,\mathrm{e}^{-i[m\theta+n\theta^*]}, \\ \text{where}\quad \Gamma_{mn}(z,z',z^*) &= \left[\frac{\partial}{\partial z'}g_m(z,z')\right]\left[\frac{\partial}{\partial z'}g_n(z',z^*)\right]-mng_m(z,z')\,g_n(z',z^*). \end{aligned}\right\} \tag{5.10}$$

Using these results and (4.17), the resistance matrix R_{ij} may be expanded in the form

$$R_{ij} = R_{ij}^{(0)} + \delta R_{ij}^{(1)} + \delta^2 R_{ij}^{(2)} + \ldots. \tag{5.11}$$

This expansion is straightforward but lengthy, and is omitted for brevity.† Several terms are evaluated as needed in the next section.

6. Motion of an axisymmetric particle due to a pressure difference

In the absence of body forces, the force driving the particle results from the pressure difference between the ends of the particle, and is in the z-direction. As discussed earlier, this pressure difference must be of order ϵ^{-1} to give an $O(1)$ particle velocity, and we may assume

$$\Delta p = p(z_+) - p(z_-) = -4\epsilon^{-1}l_0. \tag{6.1}$$

This pressure difference, while much smaller than the $O(\epsilon^{-2})$ pressures generated within the lubrication layer, appears at leading order in the axial force balance, since it acts on the ends of the particle. At leading order in ϵ, the resulting contribution to the force on the particle is $\pi\Delta p$, and the condition of zero net force on the particle then gives

$$F_3 + 4\pi l_0 = 0 \quad \text{and} \quad F_i = 0 \quad \text{for} \quad i \neq 3. \tag{6.2}$$

The particle velocity satisfies the linear system

$$\sum_{j=1}^{6} R_{ij}V_j = -4\pi l_0\,\delta_{i3}. \tag{6.3}$$

We now restrict our attention to the case in which the particle shape is axisymmetric, since this greatly simplifies the analysis. Also, we assume that the gap is almost uniform, as in the previous section. (Examples in which these assumptions are not made are considered in the next section.) Therefore, the particle has radius $1-\epsilon+\epsilon\delta s(z)$ where $s(z)$ is a prescribed function describing the shape, and where we may assume that the mean of $s(z)$ on $[-l_0, l_0]$ is zero. Furthermore, we assume for simplicity that the tube axis and the particle axis both lie in the plane $y = 0$, which is then a symmetry plane of the flow, and so $V_i = 0$ for $i = 2, 4, 6$ (see table 1). It can be shown that motion in

† Details are given in an appendix available on request from the authors or the Editor.

this plane is decoupled from motion in the plane $x = 0$, up to $O(\delta^2)$. Therefore, general particle motions may be regarded as a superposition of motions in these two planes. Under these assumptions,

$$\xi_{p1} = s(z) \quad \text{and} \quad \xi_{w1} = [a_1 + \alpha_1(z-c)]\cos\theta \tag{6.4}$$

and the only non-zero Fourier components appearing in (5.2) are

$$H_{\pm 1}(z) = a_1 + \alpha_1(z-c) \quad \text{and} \quad H_0(z) = -2s(z). \tag{6.5}$$

We expand the velocity:

$$V_i = V_i^{(0)} + \delta V_i^{(1)} + \delta^2 V_i^{(2)} + \ldots. \tag{6.6}$$

At order δ^0, it is easily shown that the resistance matrix $R_{ij}^{(0)}$ is diagonal, and that $R_{33}^{(0)} = -4\pi l_0$. Therefore,

$$V_3^{(0)} = 1 \quad \text{and} \quad V_i^{(0)} = 0 \quad \text{for} \quad i \neq 3 \tag{6.7}$$

with the choice of Δp made in (6.1).

At order δ^1, (6.3) gives

$$V_i^{(1)} = -R_{i3}^{(1)}/R_{ii}^{(0)}. \tag{6.8}$$

Now, from (4.17), (5.5) and table 1,

$$R_{13}^{(1)} = \tfrac{1}{2}\alpha_1\kappa_1, \quad R_{11}^{(0)} = -\kappa_1, \quad R_{33}^{(1)} = R_{35}^{(1)} = 0 \quad \text{and} \quad R_{55}^{(0)} = -\kappa_2, \tag{6.9}$$

where

$$\kappa_1 = -12\pi^2 \iint g_1(z, z^*)\,\mathrm{d}z\,\mathrm{d}z^* = 24\pi[l_0 - \tanh l_0]$$

and

$$\kappa_2 = -12\pi^2 \iint g_1(z, z^*)\, zz^*\,\mathrm{d}z\,\mathrm{d}z^* = 24\pi l_0[\tfrac{1}{3}l_0^2 - l_0\coth l_0 + 1]. \tag{6.10}$$

Here and below, the integrals are over $[-l_0, l_0]$. At order δ^1, therefore, the contributions to V_x, V_z and Ω_y are

$$V_1^{(1)} = \tfrac{1}{2}\alpha_1 \quad \text{and} \quad V_3^{(1)} = V_5^{(1)} = 0 \tag{6.11}$$

respectively, independent of $s(z)$.

At order δ^2, (6.3) gives

$$V_i^{(2)} = -(\tfrac{1}{2}\alpha_1 R_{i1}^{(1)} + R_{i3}^{(2)})/R_{ii}^{(0)}. \tag{6.12}$$

Now, (4.17) can be used to evaluate (6.12) for $i = 1$ and $i = 5$, leading to second-order contributions to V_x and Ω_y:

$$V_1^{(2)} = -\lambda_1(a_1 - \alpha_1 c) - \lambda_3\alpha_1 \quad \text{and} \quad V_5^{(2)} = -\lambda_2(a_1 - \alpha_1 c) - \lambda_4\alpha_1. \tag{6.13}$$

The parameters λ_i are given by

$$\lambda_i = 1/\kappa_i \int K_i(z^*)\frac{\mathrm{d}s}{\mathrm{d}z^*}\mathrm{d}z^*, \quad i = 1, 2, 3, 4, \tag{6.14}$$

where $\kappa_3 = \kappa_1$, $\kappa_4 = \kappa_2$, and

$$\left.\begin{aligned}
K_1(z^*) &= 18\pi^3 \iint \Gamma_{10}(z, z', z^*)\,\mathrm{d}z\,\mathrm{d}z' = 18\pi[1 - \cosh z^*/\cosh l_0],\\
K_2(z^*) &= 18\pi^3 \iint \Gamma_{10}(z, z', z^*)\, z\,\mathrm{d}z\,\mathrm{d}z' = 18\pi[z^* - l_0\sinh z^*/\sinh l_0],\\
K_3(z^*) &= 18\pi^3 \iint \Gamma_{10}(z, z', z^*)\, z'\,\mathrm{d}z\,\mathrm{d}z' = z^*K_1(z^*) - \tanh l_0\, K_2(z^*)/l_0,\\
K_4(z^*) &= 18\pi^3 \iint \Gamma_{10}(z, z', z^*)\, zz'\,\mathrm{d}z\,\mathrm{d}z' = z^*K_2(z^*)\\
&\quad - l_0K_1(z^*)/\tanh l_0 + 9\pi(l_0^2 - z^{*2}).
\end{aligned}\right\} \tag{6.15}$$

6.1. *Trajectories in the tube frame*

For motion in the plane $y = 0$, we may assume that $\gamma = 0$. Then, the origin of the particle and the direction of its axis are

$$(a', 0, c') = -(a - \alpha c, 0, c), \quad (\alpha', 0, 1) = (-\alpha, 0, 1) \tag{6.16}$$

in tube Cartesian coordinates at leading order in ϵ, and the consistency conditions (4.4) yield

$$\frac{da'}{dt} = V_x + \alpha' V_z, \quad \frac{dc'}{dt} = V_z, \quad \frac{d\alpha'}{dt} = \Omega_y. \tag{6.17}$$

With these relations, equations for particle trajectories may be derived.

At first order in δ (6.7) gives

$$\frac{da_1'}{dt} = \frac{\alpha_1'}{2}, \quad \frac{d\alpha_1'}{dt} = 0. \tag{6.18}$$

In this approximation, the particle moves in a straight line along the bisector of the particle and tube axes, independent of particle shape. The motion is neutrally stable with regard to exponential solutions. In general, the particle would eventually collide with the wall, in the absence of higher-order effects.

Substantially different conclusions are reached when second-order, $O(\delta^2)$, effects are included. Combining first- and second-order terms, we obtain from (6.11), (6.13) and (6.17):

$$\frac{d}{dt}\begin{bmatrix} a' \\ \alpha' \end{bmatrix} = \begin{bmatrix} \delta\lambda_1 & \frac{1}{2} + \delta\lambda_3 \\ \delta\lambda_2 & \delta\lambda_4 \end{bmatrix} \begin{bmatrix} a' \\ \alpha' \end{bmatrix} \tag{6.19}$$

neglecting $O(\delta^3)$ terms. The parameters λ_i depend on the shape of the particle according to (6.14), which may be restated in the form

$$\lambda_i = -\frac{1}{\kappa_i} \int_{-l_0}^{l_0} \frac{dK_i}{dz} s(z)\, dz, \quad i = 1, 2, 3, 4. \tag{6.20}$$

The functions dK_i/dz are plotted in figure 3 for the case $l_0 = 2$. As figure 3 indicates, dK_1/dz and dK_4/dz are odd functions of z while dK_2/dz and dK_3/dz are even functions. Therefore, if $s(z)$ is even, then $\lambda_1 = \lambda_4 = 0$, while if $s(z)$ is odd then $\lambda_2 = \lambda_3 = 0$.

For axisymmetric particles, motion along the tube axis ($a' = \alpha' = 0$) satisfies the governing equations. To analyse the stability of this motion, we compute the eigenvalues of the matrix in (6.19):

$$\left.\begin{array}{ll} \pm(\frac{1}{2}\delta\lambda_2)^{\frac{1}{2}} + \frac{1}{2}\delta(\lambda_1 + \lambda_4) + O(\delta^{\frac{3}{2}}) & \text{if} \quad \lambda_2 \neq 0; \\ \delta\lambda_1, \delta\lambda_4 & \text{if} \quad \lambda_2 = 0. \end{array}\right\} \tag{6.21}$$

Since a non-zero leading-order term ($\frac{1}{2}$) appears in only one element of the matrix, the value of λ_2 is dominant in determining the stability of the particle motion. If $\lambda_2 > 0$, corresponding to particles wider at the ends than at the middle (wasp-waisted particles), the motion is unstable, independent of the front-to-rear taper of the particle. If $\lambda_2 < 0$ (barrel-waisted particles), taper does, however, influence stability. Consideration of the location of the eigenvalues in the complex plane leads to the following cases. For each, an example of a typical particle shape is given. The 'front' of the particle is at $z = l_0$. Note that these predictions regarding stability are based on the solution up to $O(\delta^2)$. Effects of higher-order terms are considered subsequently.

(i) $\lambda_2 > 0$: unstable. Example: particle wider at the ends than at the middle.

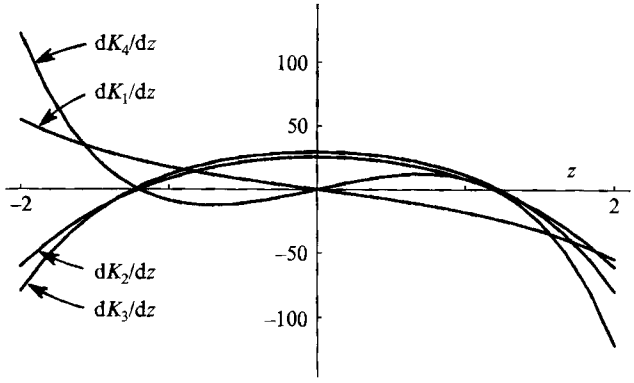

FIGURE 3. The functions dK_i/dz, $i = 2, 3, 4$, for $l_0 = 2$.

(ii) $\lambda_2 = 0$ and $\mathrm{Max}(\lambda_1, \lambda_4) > 0$: unstable. Example: uniformly tapered particle, wider at front than at rear.

(iii) $\lambda_2 = \mathrm{Max}(\lambda_1, \lambda_4) = 0$: neutrally stable. Example: perfectly cylindrical particle.

(iv) $\lambda_2 = 0$ and $\mathrm{Max}(\lambda_1, \lambda_4) < 0$: stable. Example: uniformly tapered particle, narrower at front than at rear.

(v) $\lambda_2 < 0$ and $\lambda_1 + \lambda_4 > 0$: unstable to growing oscillations. Example: particle wider at middle than at ends, and wider at front than at rear.

(vi) $\lambda_2 < 0$ and $\lambda_1 + \lambda_4 = 0$: neutrally stable (constant-amplitude oscillations). Example: particle wider at middle than at ends, and symmetric front to rear.

(vii) $\lambda_2 < 0$ and $\lambda_1 + \lambda_4 < 0$: stable. The particle undergoes decaying oscillations. Example: particle wider at middle than at ends, and narrower at front than at rear.

Since inclusion of $O(\delta^2)$ effects leads to behaviour different to that predicted by the $O(\delta)$ theory, the question arises whether $O(\delta^3)$ effects would alter these conclusions. An indication may be obtained by considering the effects of perturbing the elements in the matrix (6.19) by $O(\delta^2)$ amounts. In the general case $\lambda_2 \neq 0$, the expression (6.21) for the eigenvalues is unchanged, and so the above conclusions still hold, except that case (vi) may no longer be neutrally stable. In the special case $\lambda_2 = 0$, however, this perturbation will alter the eigenvalues (6.21) at leading order, and may affect the stability of the motion. For example, consider a uniformly tapered particle (figure 2*c*). By arguments analogous to those made in §2, sideways displacement of this particle results in an anticlockwise torque, not shown in figure 2. This torque represents an $O(\delta^3)$ correction to the term $\delta\lambda_2$ appearing in (6.19), and might therefore destabilize the motion. This case is examined in §7.

Higher-order effects for axisymmetric particles may also include coupling between the motions of the particle in two orthogonal planes containing the axis, and particle rotation about the axis. Such effects would not alter the above conclusions regarding stability. The consistency of the above predictions with the numerical results of §7 (corresponding to $O(1)$ values of δ) also suggests that the $O(\delta^2)$ analysis captures the main features of the particle behaviour.

Examples of the types of behaviour described above are obtained if the following two-parameter family of particle shapes is considered:

$$s(z) = s_1 z + s_2(\tfrac{1}{3}l_0^2 - z^2). \tag{6.22}$$

Evaluating (6.14) and substituting in (6.19), we obtain

$$\frac{\mathrm{d}}{\mathrm{d}t}\begin{bmatrix} a' \\ \alpha' \end{bmatrix} = \begin{bmatrix} \frac{3}{2}\delta s_1 & \frac{1}{2} - M\delta s_2 \\ -3\delta s_2 & 3\delta s_1 \end{bmatrix}\begin{bmatrix} a' \\ \alpha' \end{bmatrix}, \tag{6.23}$$

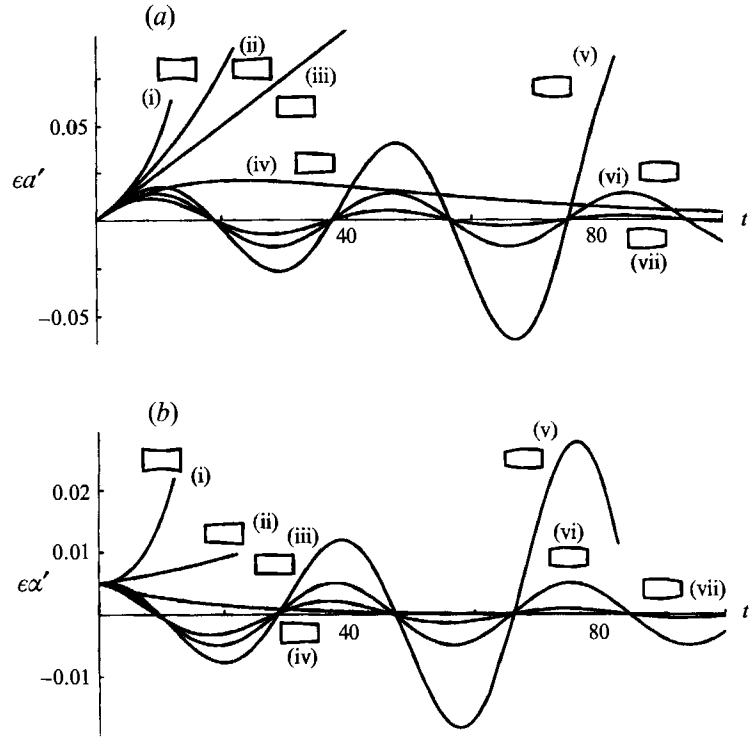

FIGURE 4. Variation with time of (*a*) particle displacement a' and (*b*) particle orientation α', as predicted by the second-order theory, for particle shapes corresponding to the cases described in the text, with $\epsilon = 0.1$: (i) $\delta s_1 = 0$, $\delta s_2 = -0.02$; (ii) $\delta s_1 = 0.01$, $\delta s_2 = 0$; (iii) $\delta s_1 = 0$, $\delta s_2 = 0$; (iv) $\delta s_1 = -0.02$, $\delta s_2 = 0$; (v) $\delta s_1 = 0.01$, $\delta s_2 = 0.02$; (vi) $\delta s_1 = 0$, $\delta s_2 = 0.02$; (vii) $\delta s_1 = -0.01$, $\delta s_2 = 0.02$. Corresponding particle shapes are indicated, with diameter variations exaggerated for clarity. In the unstable cases, curves are truncated when the particle touches the wall.

where
$$M = 9 + 4l_0^2 - 3l_0^3/[l_0 - \tanh l_0]. \tag{6.24}$$

Figure 4 shows the motion predicted by (6.23) for particle shapes in this family, with one example from each of the seven cases described above.

7. Numerical solutions

If the gap is not almost uniform, the series expansion may not yield a good approximation. For such cases, we used a numerical solution. In all cases considered, the flow is symmetric about the plane $y = 0$, and so the only non-zero components of forces, torques and velocities are for $i = 1, 3$ and 5 (see table 1). The equation

$$\mathrm{L}(P) = W_i(z, \theta)$$

was expressed in finite-difference form using centred differences, and solved by successive over-relaxation for $i = 1, 3, 5$. By symmetry, only the region $\{0 \leqslant \theta \leqslant \pi\}$ was considered. A 20×20 grid was used for most calculations, and selected cases were repeated using finer grids to check the results. For each value of i, the three non-zero components of force and moment were then computed by integrating (4.12) using the trapezium rule, giving the non-zero components of the resistance matrix R_{ij}. Equation (6.3) was solved to yield particle velocities, and particle trajectories were computed by integrating (6.17) using a fourth-order Runge–Kutta scheme.

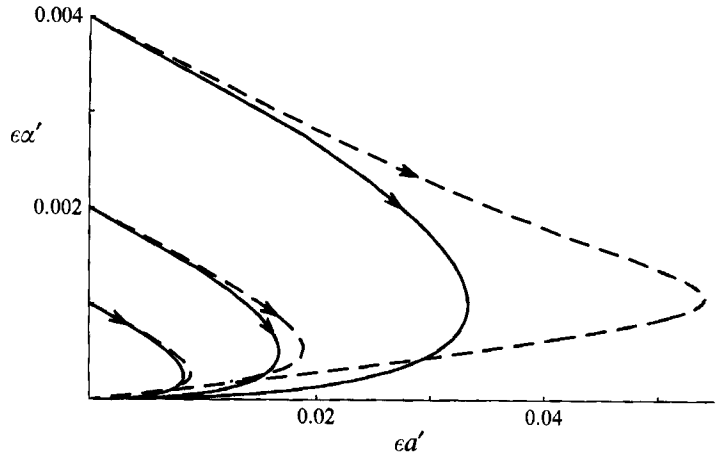

FIGURE 5. Trajectories in the (a', α')-plane for a conical particle, narrower at the front ($\epsilon = 0.1$, $\delta s_1 = -0.01$, $\delta s_2 = 0$), initially centred on but inclined relative to the tube axis, for several different initial inclinations: ——, second-order theory; – – – –, numerical method.

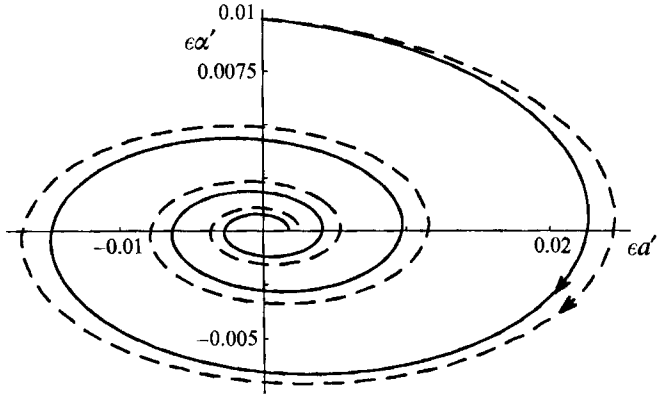

FIGURE 6. Trajectories in the (a', α')-plane for a particle which is wider in the middle than the ends, and narrower at the front than at the rear ($\epsilon = 0.1$, $\delta s_1 = -0.01$, $\delta s_2 = 0.02$), initially centred on but inclined relative to the tube axis: ——, second-order theory; – – – –, numerical method.

Figure 5 shows a comparison of results from the series method and the numerical solution for a slightly tapered conical particle, narrower at the front, initially centred on but not aligned with the axis. In this case, $\epsilon = 0.1$, and so $\epsilon a' = 0.05$ corresponds to a 50% change in the gap width. Note that according to the first-order $[O(\delta)]$ theory, α' would remain constant and the particle would eventually collide with the wall. The $O(\delta^2)$ prediction that the particle will eventually approach axial position ($\alpha' = a' = 0$) is supported by the numerical results, implying that higher-order terms do not, in fact, destabilize the motion. For small starting angles, the series approach provides a fair approximation to the trajectory, but for a starting angle of $\epsilon\alpha' = 0.004$, the series approach substantially underestimates the maximum excursion made by the particle. The $O(\delta^2)$ theory predicts that the particle trajectory approaches the origin along the $\epsilon a'$-axis. However, the numerically computed final approach to the origin is along a line at an angle to the $\epsilon a'$-axis, as a result of the $O(\delta^3)$ effects mentioned previously.

Corresponding results are shown in figure 6 for the case of a particle which is wider at the middle than at the ends, and wider at the front than at the rear. The series

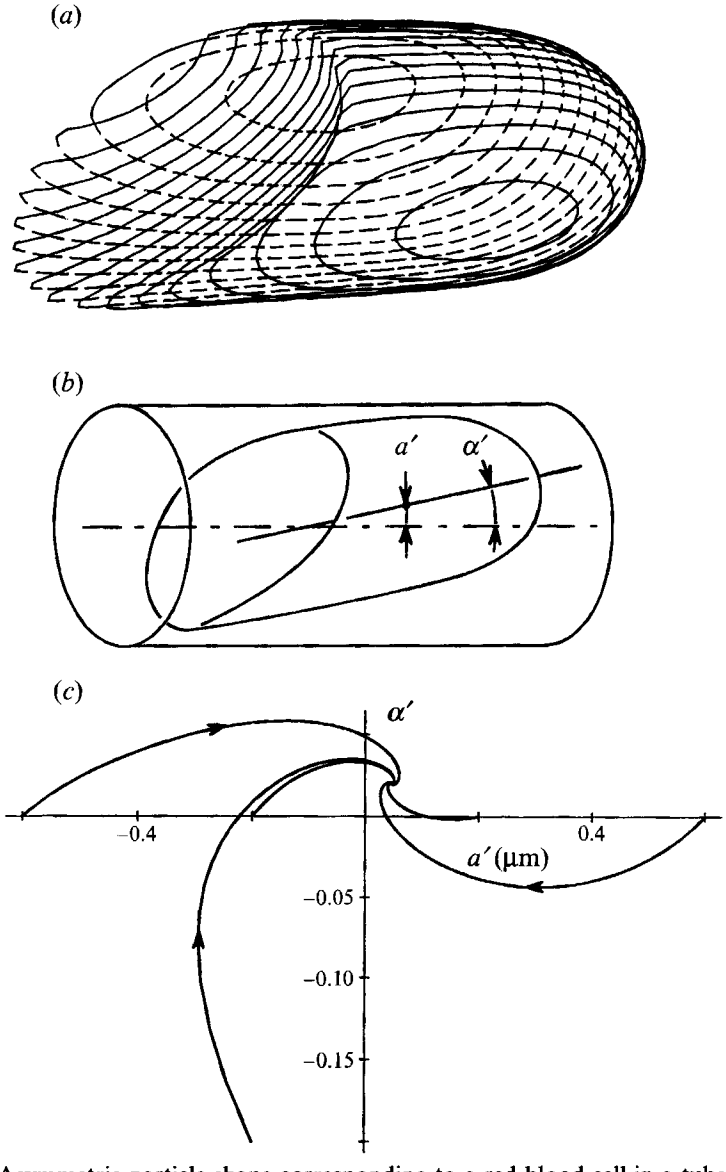

FIGURE 7. (*a*) Asymmetric particle shape corresponding to a red blood cell in a tube with diameter 6 μm. (*b*) Parameters describing particle position in the tube. Note that a' and α' are not scaled as elsewhere. (*c*) Particle trajectories in the (a', α')-plane, for several different initial conditions.

solution correctly predicts the qualitative behaviour, and provides a good approximation to the motion.

Numerical results are shown in figure 7 for a rigid particle with a shape corresponding to experimentally observed asymmetric red blood cells (Hsu & Secomb, 1989). For motion in the observed flow direction, the particle undergoes decaying oscillations, corresponding to case (vii) above. Because of the non-axisymmetry of the particle, the equilibrium solution is no longer at $a' = \alpha' = 0$. Note that if the flow direction is reversed, the equilibrium solution for a rigid particle with this shape is unstable to growing oscillations. Since the particle is wider in the middle than at the ends, the oscillatory motion is consistent with the predictions of the series method. However, the

series method as developed above is not directly applicable to particles such as this red cell shape for which the gap length varies around the circumference of the particle (i.e. z_+ and z_- are not constants). Further work is required to develop general criteria for the stability of such particles' motions. It should be emphasized that red blood cells are actually highly deformable, and that deformability may influence the stability of particle motions. Therefore, the present results are not directly applicable to the motion of red cells.

8. Discussion and conclusions

A striking conclusion of these studies is that the trajectories of rigid closely fitting particles in cylindrical tubes are highly sensitive to the shape of the particle and the flow direction. In the case of an axisymmetric particle, motion along the tube axis represents an equilibrium solution of the governing equations. In general, this equilibrium is unstable if the particle is narrower near the middle than the average of the two ends, or more precisely if λ_2 is positive according to (6.20). Otherwise, the equilibrium is stable if the leading end of the particle is narrower than the trailing end, and unstable if the leading end is larger, as defined by the signs of λ_1 and λ_4.

In the case of unstable motions, the series method predicts unbounded increase in particle displacement, which in reality is clearly limited by the physical constraint that the particle cannot intersect the tube wall. The eventual behaviour in such cases is unknown. If the particle has sharp corners at its ends, the lubrication approximation may break down when one of these corners closely approaches the tube wall, and the subsequent behaviour will depend on the detailed mechanics in the neighbourhood of the corner. If, on the other hand, the particle has a smooth profile, like the red-cell shape assumed, the series method may break down while the lubrication approximation remains valid. The motion in such cases could, in principal, be predicted using our numerical approach, but refinement of the mesh would be required.

Some related experimental studies have been made. Boyd (1964) demonstrated qualitatively the effect of taper on the 'sticking' of pistons, but did not consider pistons with curved profiles. Hochmuth & Sutera (1970) reported that spherical caps flowing in tubes generally tend to align themselves with their curved surfaces facing in the direction of flow. However, neither of these studies provides a direct test of the results presented here.

Few previous theoretical studies have been made of the non-axisymmetric creeping flow of non-spherical particles in fluid-filled tubes, probably because of the difficulties involved in solving fully three-dimensional Stokes flow problems. Use of lubrication theory greatly simplifies the governing equations, while permitting consideration of a variety of particle shapes, subject to the constraint that the particles fit closely in the tube. It would be of great interest to determine whether the conclusions stated above, regarding the stability of particle motions, generalize to particles that are not closely fitting.

This work was supported by NIH Grants HL34555 and HL07249. We thank several referees for helpful suggestions.

REFERENCES

BARNARD, A. C. L., LOPEZ, L. & HELLUMS, J. D. 1968 Basic theory of blood flow in capillaries. *Microvasc. Res.* **1**, 23–34.

BOYD, J. 1964 The influence of fluid forces on the sticking and the lateral vibration of pistons. *Trans. ASME* E: *J. Appl. Mech.* **31**, 397–401.

BUNGAY, P. M. & BRENNER, H. 1973 The motion of a closely-fitting sphere in a fluid-filled tube. *Intl J. Multiphase Flow* **1**, 25–56.

CAMERON, A. 1966 *The Principles of Lubrication.* Wiley.

CHEN, T. C. & SKALAK, R. 1970 Stokes flow in a cylindrical tube containing a line of spheroidal particles. *Appl. Sci. Res.* **22**, 403–441.

CHRISTOPHERSON, D. G. & DOWSON, D. 1959 An example of minimum energy dissipation in viscous flow. *Proc. R. Soc. Lond.* A **251**, 550–564.

GOLDMAN, A. J., COX, R. G. & BRENNER, H. 1967 Slow viscous motion of a sphere parallel to a plane wall. I. Motion through a quiescent fluid. *Chem. Engng Sci.* **22**, 637–651.

HAPPEL, J. & BRENNER, H. 1973 *Low Reynolds Number Hydrodynamics* 2nd revised edn. Noordhoff.

HOCHMUTH, R. M. & SUTERA, S. P. 1970 Spherical caps in low Reynolds-number flow. *Chem. Engng Sci.* **25**, 593–604.

HSU, R. & SECOMB, T. W. 1989 Motion of non-axisymmetric red blood cells in cylindrical capillaries. *J. Biomech. Engng* **111**, 147–151.

LEAL, L. G. 1980 Particle motions in a viscous fluid. *Ann. Rev. Fluid Mech.* **12**, 435–476.

LIGHTHILL, M. J. 1968 Pressure-forcing of tightly fitting pellets along fluid-filled elastic tubes. *J. Fluid Mech.* **34**, 113–143.

SECOMB, T. W. & SKALAK, R. 1982 A two-dimensional model for capillary flow of an asymmetric cell. *Microvasc. Res.* **24**, 194–203.

SECOMB, T. W., SKALAK, R., ÖZKAYA, N. & GROSS, J. F. 1986 Flow of axisymmetric red blood cells in narrow capillaries. *J. Fluid Mech.* **163**, 405–423.

SUGIHARA-SEKI, M., SECOMB, T. W. & SKALAK, R. 1990 Two-dimensional analysis of two-file flow of red cells along capillaries. *Microvasc. Res.* **40**, 379–393.

TÖZEREN, H. & SKALAK, R. 1978 The steady flow of closely fitting incompressible elastic spheres in a tube. *J. Fluid Mech.* **87**, 1–16.

WAKIYA, S. 1957 Viscous flows past a spheroid. *J. Phys. Soc. Japan* **12**, 1130–1141.

ZARDA, P. R., CHIEN, S. & SKALAK, R. 1977 Interaction of viscous incompressible fluid with an elastic body. In *Computational Methods for Fluid-Solid Interaction Problems* (ed. T. Belytschko & T. L. Geers), pp. 65–82. ASME.